Defective BN Nanotubes: A Density Functional Theory Study of B-11 and N-14 NQR Parameters

Masoud Giahi[a] and Mahmoud Mirzaei[b]

[a] Department of Chemistry, Lahijan Branch, Islamic Azad University, Lahijan, Iran
[b] Department of Chemistry, Shahr-e-Rey Branch, Islamic Azad University, Shahr-e-Rey, Iran

Reprint requests to M. M.; E-mail: mdmirzaei@yahoo.com

Z. Naturforsch. **64a,** 251 – 256 (2009); received January 23, 2008 / revised June 23, 2008

A density functional theory (DFT) study is performed to investigate the influence of structural defects on the electronic structure properties of perfect boron nitride nanotubes (BNNTs). To this aim, as representative models, the single-walled (6,0) BNNT consisting of 36 boron, 36 nitrogen, and 12 hydrogen atoms and the single-walled (4,4) BNNT consisting of 36 boron, 36 nitrogen, and 16 hydrogen atoms are considered. The nuclear quadrupole resonance (NQR) parameters are calculated and compared in two perfect and defective models of the considered BNNTs. The results indicate that due to formation of non-hexagonal rings in the defective model because of removing a B – N bond, the NQR parameters at the sites of first neighbouring nuclei are significantly influenced by imposed perturbation, however, the sites of other nuclei, farther from perturbation, remain almost unchanged. The calculations are performed at the level of the BLYP method and 6-31G* standard basis set using the GAUSSIAN 98 package.

Key words: Defect; Boron Nitride; Nanotube; Electric Field Gradient; DFT.

1. Introduction

Very soon after the discovery of carbon nanotubes (CNTs) [1], numerous studies have been devoted to investigate the properties and applications of the fascinating novel material [2, 3]. The applications of CNTs range from nanoelectronics to nanobiotechnology, e. g., they are used as either electronic field emitters or artificial muscles [4, 5]. Depending upon the tubular diameter and chirality, CNTs exhibit metallic or semiconducting behaviour, hence, it is a difficult task to synthesize them for the desired purposes [6]. Therefore, considerable efforts have been made to synthesize non-carbon inorganic nanotubes with properties independent of the tubular diameter and chirality. The group III nitride nanotubes, especially boron nitride nanotubes (BNNTs), are viewed as proper alternative materials which exhibit semiconducting behaviour [7 – 9]. Since B and N are the first neighbours of C in the periodic table, the total number of electrons in the valence shells of one B and one N atom is equal to that of two C atoms. Both the electronic structure and the characteristic semiconducting behaviour make BNNTs an interesting subject of numerous studies [10 – 12]. The stable one-dimensional structure of BNNTs was first recognized theoretically and then BNNTs were successfully synthesized [13, 14].

Nuclear quadrupole resonance (NQR) spectroscopy is an insightful technique to study the physical properties of matter in solidphase [15]. The parameters measurable by are the quadrupole coupling constant (C_Q) and asymmetry parameter (η_Q) which both are also reproducable by quantum chemical calculations of the electric field gradient (EFG) tensors. The EFG tensors originated at the sites of quadrupole nuclei, the nuclei with nuclear spin angular momentum greater that one ($I > 1$), e. g. ^{11}B and ^{14}N, are very sensitive to the electronic density at the sites of nuclei and feel changes by any perturbation [16, 17]. In this work, by the advantage of EFG tensor calculations, structural defects in representative models of the single-walled zigzag and armchair BNNTs are studied at the level of the density functional theory (DFT). To this aim, the EFG tensors at the sites of various ^{11}B and ^{14}N nuclei in two perfect (Figs. 1 and 3) and defective (Figs. 2 and 4) models of (6,0) and (4,4) single-walled BNNTs are calculated (Tables 1 – 4) to indicate to which extend the electronic structure properties of BNNTs are influenced by defects. The presence of defects in nanotubes causes important applications, e. g. as hydrogen storage material [18].

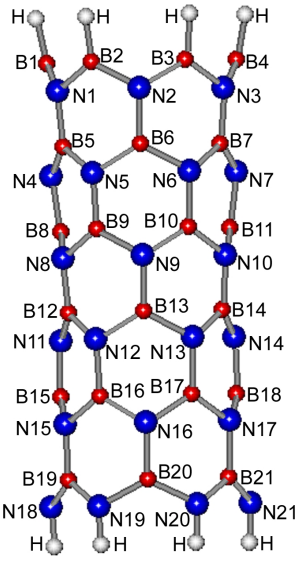

Fig. 1. The 2D view of perfect (6,0) zigzag BNNT.

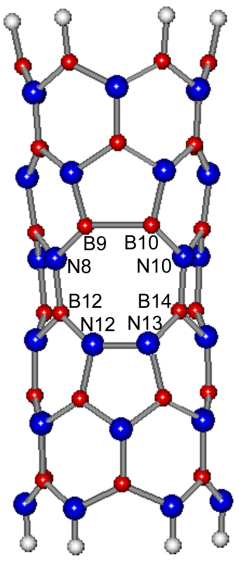

Fig. 2. The 2D view of defective (6,0) zigzag BNNT.

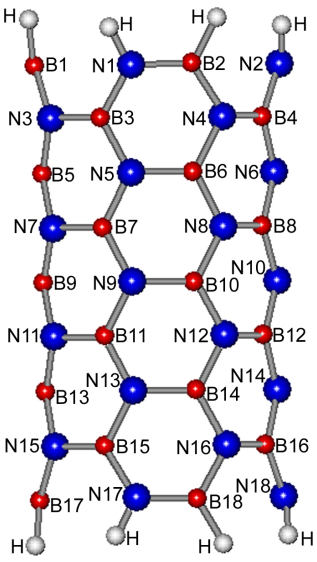

Fig. 3. The 2D view of perfect (4,4) armchair BNNT.

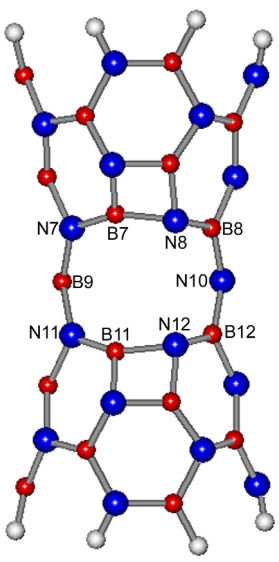

Fig. 4. The 2D view of defective (4,4) armchair BNNT.

2. Computational Aspects

2.1. Preparation of Models

The models considered in the present study are the single-walled zigzag and armchair BNNTs. As a representative model of the single-walled zigzag BNNTs, a 14-Å length of a (6,0) model consisting of 36 B and 36 N atoms in which the two ends of the tube are saturated by 12 H atoms is considered (Fig. 1). In addition, a B – N bond, B13 – N9, is removed from the centre of the perfect model to create a defective model consisting of 35 B, 35 N, and 12 H atoms (Fig. 2). As a representative perfect model of the single-walled armchair BNNTs, a 12-Å length of a (4,4) model consisting of 36 B, 36 N, and 16 H atoms is considered (Fig. 3). A B – N bond, B10 – N9, is also removed from the centre of the perfect model to create a defective model consisting of 35 B, 35 N, and 16 H atoms (Fig. 4). It is worth noting that the validity of the considered BNNT model concerning tube length and number of atoms for theoretical calculations was examined in [18]. As a first step of the present study, both models are individually optimized at the level of the DFT employing the BLYP method and 6-31G* standard basis set. All quantum chemical calculations are performed using the GAUSSIAN 98 package of program [19].

2.2. Calculation of Parameters

As the second step of the present study, the EFG tensors at the sites of various ^{11}B and ^{14}N nuclei are calculated by employing the BLYP method and 6-31G* standard basis set in each of the two optimized perfect and defective models. Directly relating to the experiments, the calculated EFG tensors are converted to measurable NQR parameters, i. e. the quadrupole coupling constant (C_Q) and asymmetry parameter (η_Q)

$$C_Q\,(\mathrm{MHz}) = e^2 Q q_{zz} h^{-1}, \tag{1}$$

$$\eta_Q = |(q_{xx} - q_{yy})/q_{zz}|. \tag{2}$$

C_Q is the interaction energy between the EFG tensors and the electric nuclear quadrupole moment (eQ), while η_Q is a measure of the EFG tensors' deviation from cylindrical symmetry at the site of the quadrupole nucleus. It has to be noted that the EFG tensors are originated at the sites of quadrupole nuclei, e. g. ^{11}B and ^{14}N, where the nuclear spin angular momentum is greater than one ($I > 1$) [20]. The standard values of Q reported by Pyykkö [21] are employed in (1), $Q(^{11}\mathrm{B}) = 40.59$ mb and $Q(^{14}\mathrm{N}) = 20.44$ mb. The evaluated NQR parameters at the sites of various ^{11}B and ^{14}N nuclei for the perfect and defective models of BNNTs are listed in Tables 1 – 4.

Table 1. The boron-11 NQR parameters of zigzag BNNT.

Layer	Nucleus	C_Q (MHz)		η_Q	
		Perfect[a]	Defective[b]	Perfect[a]	Defective[b]
1	B1	3.58	3.59	0.30	0.29
	B2	3.58	3.58	0.30	0.30
	B3	3.58	3.58	0.30	0.30
	B4	3.58	3.59	0.30	0.29
2	B5	2.79	2.75	0.11	0.08
	B6	2.79	2.91	0.11	0.12
	B7	2.79	2.75	0.11	0.08
3	B8	2.76	2.76	0.09	0.10
	B9	2.76	3.51	0.09	0.29
	B10	2.76	3.51	0.09	0.29
	B11	2.76	2.76	0.09	0.10
4	B12	2.75	2.78	0.08	0.11
	B13	2.75	–	0.08	–
	B14	2.75	2.78	0.08	0.11
5	B15	2.74	2.68	0.08	0.08
	B16	2.74	2.50	0.08	0.06
	B17	2.74	2.50	0.08	0.06
	B18	2.74	2.68	0.08	0.08
6	B19	2.56	2.55	0.14	0.11
	B20	2.56	2.60	0.14	0.15
	B21	2.56	2.55	0.14	0.11

[a] Fig. 1. [b] Fig. 2.

Table 2. The nitrogen-14 NQR parameters of zigzag BNNT.

Layer	Nucleus	C_Q (MHz)		η_Q	
		Perfect[a]	Defective[b]	Perfect[a]	Defective[b]
1	N1	0.93	0.95	0.44	0.48
	N2	0.93	1.00	0.44	0.31
	N3	0.93	0.95	0.44	0.48
2	N4	0.96	0.82	0.08	0.21
	N5	0.96	0.84	0.08	0.38
	N6	0.96	0.84	0.08	0.38
	N7	0.96	0.82	0.08	0.21
3	N8	1.00	0.48	0.01	0.91
	N9	1.00	–	0.01	–
	N10	1.00	0.48	0.01	0.91
4	N11	1.01	1.17	0.01	0.23
	N12	1.01	5.17	0.01	0.68
	N13	1.01	5.17	0.01	0.68
	N14	1.01	1.17	0.01	0.23
5	N15	1.05	1.00	0.06	0.18
	N16	1.05	0.65	0.06	0.39
	N17	1.05	1.00	0.06	0.18
6	N18	2.43	2.46	0.84	0.84
	N19	2.43	2.46	0.84	0.80
	N20	2.43	2.46	0.84	0.80
	N21	2.43	2.46	0.84	0.84

[a] Fig. 1. [b] Fig. 2.

3. Results and Discussion

3.1. The ^{11}B NQR Parameters

The calculated EFG tensors at the sites of various ^{11}B nuclei in each of the two considered perfect and defective models of zigzag and armchair BNNTs (Figs. 1 – 4) are converted to measurable NQR parameters, the quadrupole coupling constant (C_Q) and asymmetry parameter (η_Q) (Tables 1 and 3). For the zigzag BNNT (Table 1), the calculated NQR parameters at the sites of various ^{11}B nuclei are divided into six layers where the nuclei in the perfect model (Fig. 1) have almost the same electrostatic environment resulting in

Table 3. The boron-11 NQR parameters of armchair BNNT.

Layer	Nucleus	C_Q (MHz)		η_Q	
		Perfect[a]	Defective[b]	Perfect[a]	Defective[b]
1	B1	3.15	3.14	0.17	0.16
	B2	3.15	3.11	0.17	0.24
2	B3	2.72	2.84	0.03	0.08
	B4	2.72	2.66	0.03	0.06
3	B5	2.72	2.55	0.05	0.11
	B6	2.72	2.73	0.05	0.04
4	B7	2.72	2.71	0.05	0.11
	B8	2.72	2.89	0.05	0.07
5	B9	2.71	2.53	0.06	0.03
	B10	2.71	–	0.06	–
6	B11	2.72	2.71	0.05	0.11
	B12	2.72	2.89	0.05	0.07
7	B13	2.72	2.55	0.05	0.11
	B14	2.72	2.73	0.05	0.04
8	B15	2.72	2.84	0.03	0.08
	B16	2.72	2.66	0.03	0.06
9	B17	3.15	3.14	0.17	0.16
	B18	3.15	3.11	0.17	0.24

[a] Fig. 3. [b] Fig. 4.

Table 4. The nitrogen-14 NQR parameters of armchair BNNT.

Layer	Nucleus	C_Q (MHz)		η_Q	
		Perfect[a]	Defective[b]	Perfect[a]	Defective[b]
1	N1	1.77	1.75	0.79	0.98
	N2	1.77	1.75	0.79	0.70
2	N3	0.81	0.73	0.73	0.45
	N4	0.81	1.04	0.73	0.37
3	N5	0.68	0.35	0.68	0.63
	N6	0.68	0.67	0.68	0.36
4	N7	0.74	1.48	0.52	0.01
	N8	0.74	1.10	0.52	0.72
5	N9	0.66	–	0.59	–
	N10	0.66	0.42	0.59	0.07
6	N11	0.74	1.48	0.52	0.01
	N12	0.74	1.10	0.52	0.72
7	N13	0.68	0.35	0.68	0.63
	N14	0.68	0.67	0.68	0.36
8	N15	0.81	0.73	0.73	0.45
	N16	0.81	1.04	0.73	0.37
9	N17	1.77	1.75	0.79	0.98
	N18	1.77	1.75	0.79	0.70

[a] Fig. 3. [b] Fig. 4.

the same NQR parameters. However, this harmony is perturbed in the defective model (Fig. 2) by removing the B13 – N9 bond from the perfect model. In the perfect model, the magnitude of C_Q at the sites of ^{11}B nuclei in layer 1 is largest and that of layer 6 is smallest among all layers. BNNTs have two different ends where the magnitude of $C_Q(^{11}B)$ decreases from the B end to the N end revealing importance to the nuclei in the ends of nanotubes [22]. Furthermore, the observed difference in the magnitudes of $C_Q(^{11}B)$ in layers 2 to 5 is almost negligible, however, the difference in comparison with layers 1 and 6 is significant. Removing a B – N bond, B13 – N9, leads to an octagonal ring in the defective model (Fig. 2) which causes a perturbation in the electronic structure of the perfect BNNT. Therefore, comparison of the NQR parameters at the sites of ^{11}B nuclei in various layers of the perfect and defective models reveals significant differences in the calculated parameters due to the imposed perturbation. However, it is worth noting that the significance of the imposed perturbation is just for the nuclei in the first neighbourhood layer of the octagonal ring and the electronic environment at the sites of those ^{11}B nuclei farther away from the octagonal ring do not feel the perturbation effects. In addition to the octagonal ring, two pentagonal rings also result in the defective model by removing the bond B13 – N9. In the perfect model, each B is bound to N, however, B9 and B10 are directly bound in the defective model. Therefore, C_Q of ^{11}B9 and ^{11}B10 increases by 0.75 MHz and η_Q by 0.20 from the perfect model to the defective model. In contrast with this significant difference, the NQR parameters of ^{11}B12 and ^{11}B14 do not change due to imposed perturbation in the defective model. B9 and B10 are also bound in the upper pentagonal ring in the defective model; therefore, C_Q of ^{11}B6, another boron atom in the upper pentagonal ring, increases by 0.12 MHz from the perfect to the defective model. In contrast with the lower pentagonal ring, C_Q of ^{11}B16 and ^{11}B17 decreases by 0.24 MHz from the perfect to the defective model. This trend is caused by the different electronic environments at the sites of the B nuclei in the two pentagonal rings where in the lower ring two nitrogen are directly bound. A recent study [22] indicated that when a ring in a BNNT is doped by carbon atoms, those nuclei which are locate at the first neighbourhood of the doped ring show properties similar to the end nuclei. Our present results also show that C_Q of ^{11}B9 and ^{11}B10 which are directly influenced by perturbation in the defective model is almost the same as C_Q of ^{11}B at the B end of the perfect model.

For the armchair BNNT (Table 3), some differences are observed in comparison with the zigzag model. There are two different B and N ends in zigzag BNNTs (Fig. 1); however, the two ends of armchair BNNTs are similar to each other (Fig. 3) yielding similar calculated NQR parameters at the two ends. The calculated ^{11}B NQR parameters are divided into nine layers with equivalent electrostatic properties at the sites of the nuclei in each layer. Both layers 1 and 9 are placed at the ends of the considered armchair BNNT with the same calculated NQR parameters; $C_Q(^{11}B) = 3.15$ MHz and $\eta_Q(^{11}B) = 0.17$. With the exception of the ends of the nanotube, layers 1 and 9, the calculated NQR parameters of all other layers are similar revealing the importance of the ends of the nanotubes in their behaviours and applications. The $C_Q(^{11}B)$ value of layer 5, in the middle of the nanotube, is 2.71 MHz which is the smallest value among the other layers. When a B – N bond, B10 – N9, is removed in the defective armchair model (Fig. 4), two tetragonal rings and one decagonal ring result instead of three hexagonal rings. This structural defect significantly perturbs the electronic density at the sites of those ^{11}B nuclei located in the nearest neighbourhood of the new tetragonal and decagonal rings; however, those ^{11}B nuclei located at greater distance are not affected significantly by the imposed perturbation. Layers 1 and 9 still have the largest values of $C_Q(^{11}B)$ close to the value of the perfect model, while layer 5 has the smallest value, 0.18 MHz smaller than that of the perfect model. The electronic sites of B8 and B12 in layers 4 and 6 are significantly influenced yielding in an increase of 0.17 MHz in the value of $C_Q(^{11}B)$ in comparison with the perfect model. A reverse influence is also observed at the electronic sites of B5 and B13 in layers 3 and 7 where the $C_Q(^{11}B)$ value decreases by 0.17 MHz in comparison with the perfect model. The results reveal that the imposed perturbation has significant influence on the magnitude of the EFG tensors yielding different values of $C_Q(^{11}B)$ and less influence on the deviations of the EFG tensors from cylindrical symmetry yielding almost to similar values of $\eta_Q(^{11}B)$.

3.2. The ^{14}N NQR Parameters

The calculate EFG tensors at the sites of various ^{14}N nuclei in the perfect and defective models of zigzag and armchair BNNTs are converted to measur-

able NQR parameters (C_Q and η_Q); they are listed in Tables 2 and 4. Parallel to the previous section, the calculated NQR parameters at the sites of ^{14}N nuclei in the perfect zigzag model are divided into six equivalent layers; the magnitude of C_Q in layer 6, N end, is largest and that of the opposite side, layer 1, is smallest among all layers of ^{14}N nuclei in the perfect armchair model. Except for layer 6, N end, no significant difference is observed in the C_Q values of the different layers of N nuclei. The C_Q values of N12 and N13 which are directly bound in the defective model significantly increases by 4.16 MHz from the perfect to the defective model. The magnitude of C_Q for these two N nuclei is also larger than C_Q of the N nuclei in layer 6, N end, of the perfect model. The η_Q value of N12 and N13 also reveals that the EFG tensors are fully deviated from cylindrical symmetry at the sites of these two ^{14}N nuclei in the defective model. Since N has a lone electron pair, the electron density at the site of the N nucleus is more influenced by perturbations compared with the B nucleus. The EFG tensors at the sites of ^{14}N8 and ^{14}N10 nuclei in the octagonal ring are significantly influenced due to the imposed perturbation, and C_Q decreases by 0.52 MHz and η_Q increases by 0.90 from the perfect model to the defective model. In the lower pentagonal ring of the defective model, in addition to N12 and N13, the NQR parameters of N16 are also significantly influenced; the C_Q value decreases by 0.40 MHz and η_Q increases by 0.33 from the perfect model to the defective model. In the upper pentagonal ring, the NQR parameters of N5 and N6 and also their neighbours, N4 and N7, are significantly influenced by the perturbation imposed to the electronic structure of the perfect BNNT. It is worth noting that the NQR parameters at the sites of both B and N nuclei in the back side of the defective BNNT are the same as those for the perfect BNNT revealing that the imposed perturbation just influences the first neighbours of the octagonal ring in the defective BNNT.

In perfect model of the armchair BNNT (Fig. 3), the calculated ^{14}N NQR parameters are divided into nine equivalent layers with similar electrostatic properties at the sites of ^{14}N nuclei of each layer. Layers 1 and 9 which are located at the ends of the nanotube have the largest $C_Q(^{14}N)$ value of 1.77 MHz, while layer 5 in the middle of the nanotube has the smallest value of 0.66 MHz. In contrast with the B layers, different $C_Q(^{14}N)$ values are calculated for various N layers which is mainly due to the lone electron pair in the valence shell of nitrogen. It has to be noted that the values in each layer are the same. By removing the B10 – N9 bond in the defective model of the armchair BNNT (Fig. 4), the EFG tensors at the sites of ^{14}N nuclei near the tetragonal and decagonal rings are changed. The $C_Q(^{14}N)$ values of layers 1 and 9 remain almost unchanged compared with the perfect model, however, that of layer 5 significantly decreases by 0.24 MHz. The $C_Q(^{14}N)$ values of N3, N5, N13, and N15 also decrease while those of layers 4 and 6 and N4 and N16 in layers 2 and 8 significantly increase in comparison with the perfect model. The changes of the C_Q values, reduction or increment, directly refer to changes of the electron density at the site of nuclei due to the imposed perturbation. The ends of nanotubes are very important for determining their behaviours and applications. In the defective model, the C_Q values at the sites of some N nuclei increase up to those values at the end of the nanotube revealing that the active sites of the considered BNNT are increased in the defective model.

3.3. Comparison of Zigzag and Armchair BNNTs

The atomic arrangements in zigzag and armchair BNNTs are different. Therefore, some different results are observed for these two types. In the defective model, the EFG tensors at the sites of nuclei near the imposed perturbation rings are more influenced in zigzag rather than armchair BNNTs. The C_Q values of some ^{11}B and ^{14}N nuclei near the defect increase up to those of the end of the nanotube in the zigzag model, however, this effect is just observed for some ^{14}N nuclei in the armchair model. This trend reveals that the defective zigzag BNNT has more active sites rather than the defective armchair BNNT.

4. Concluding Remarks

We calculated the NQR parameters (C_Q and η_Q) at the sites of various ^{11}B and ^{14}N nuclei using the perfect and defective models of zigzag and armchair BNNTs to study the influence of defects on the electronic structure properties of BNNTs. The results indicated that in the perfect model, the NQR parameters are divided into equivalent layers where the largest C_Q values belong to the nuclei located at the B or N end. However, this harmony is interrupted by an imposed perturbation in the defective model where the C_Q values of those B nuclei bound in an octagonal ring are equal to that of the B end and those of bound N nuclei are even remarkably

larger than that of the N end in the zigzag BNNT. On the other hand, just the C_Q values of the N nuclei undergo some increase in the armchair BNNT. This trend means that the active sites are more increased in the defective model of the zigzag BNNT than in the armchair one.

[1] S. Iijima, Nature **354**, 2148 (1991).
[2] E. Zurek and J. Autschbach, J. Am. Chem. Soc. **126**, 13079 (2004).
[3] A. Nojeh, G. W. Lakatos, S. Peng, K. Cho, and R. F.W. Pease, Nano Lett. **3**, 1187 (2003).
[4] O. Zhou, H. Shimoda, B. Gao, S. Oh, L. Fleming, and G. Yue, Acc. Chem. Res. **35**, 1045 (2002).
[5] R. H. Baughman, C. Cui, A. A. Zakhidov, Z. Iqbal, J. N. Barisci, G. M. Spinks, G. G. Wallace, A. Mazzoldi, D. De Rossi, A. G. Rinzler, O. Jaschinski, S. Roth, and M. Kertesz, Science **284**, 1340 (1999).
[6] P. J. F. Harris, Carbon Nanotubes and Related Structures, Cambridge University Press, Cambridge 1999.
[7] A. Loiseau, F. Willaime, N. Demoncy, N. Schramcheko, G. Hug, C. Colliex, and H. Pascard, Carbon **36**, 743 (1998).
[8] X. Chen, J. Ma, Z. Hu, Q. Wu, and Y. Chen, J. Am. Chem. Soc. **127**, 17144 (2005).
[9] D. Zhang and R. Q. Zhang, Chem. Phys. Lett. **371**, 426 (2003).
[10] S. Hou, Z. Shen, J. Zhang, X. Zhao, and Z. Xue, Chem. Phys. Lett. **393**, 179 (2004).
[11] M. Zhang, Z.-M. Su, L.-K. Yan, Y.-Q. Qiu, G.-H. Chen, and R.-S. Wang, Chem. Phys. Lett. **408**, 145 (2005).
[12] Ş. Erkoç, J. Mol. Struct. (Theochem.) **542**, 89 (2001).
[13] A. Rubio, J. L. Corkill, and M. L. Cohen, Phys. Rev. B **49**, 5081 (1994).
[14] N. G. Chopra, R. J. Luyken, K. Cherrey, V. H. Crespi, M. L. Cohen, S. G. Louie, and A. Zettl, Science **269**, 966 (1995).
[15] T. P. Das and E. L. Han, Nuclear Quadrupole Resonance Spectroscopy, Academic Press, New York 1958.
[16] M. Mirzaei and N. L. Hadipour, J. Phys. Chem. A **110**, 4833 (2006).
[17] M. Mirzaei and N. L. Hadipour, J. Comput. Chem. **29**, 832 (2008).
[18] H. S. Kang, J. Phys. Chem. B **110**, 4621 (2006).
[19] M. J. Frisch, G. W. Trucks, H. B. Schlegel, G. E. Scuseria, M. A. Robb, J. R. Cheeseman, V. G. Zakrzewski, J. A. Montgomery, Jr., R. E. Stratmann, J. C. Burant, S. Dapprich, J. M. Millam, A. D. Daniels, K. N. Kudin, M. C. Strain, O. Farkas, J. Tomasi, V. Barone, M. Cossi, R. Cammi, B. Mennucci, C. Pomelli, C. Adamo, S. Clifford, J. Ochterski, G. A. Petersson, P. Y. Ayala, Q. Cui, K. Morokuma, D. K. Malick, A. D. Rabuck, K. Raghavachari, J. B. Foresman, J. Cioslowski, J. V. Ortiz, A. G. Baboul, B. B. Stefanov, G. Liu, A. Liashenko, P. Piskorz, I. Komaromi, R. Gomperts, R. L. Martin, D. J. Fox, T. Keith, M. A. Al-Laham, C. Y. Peng, A. Nanayakkara, C. Gonzalez, M. Challacombe, P. M.W. Gill, B. Johnson, W. Chen, M. W. Wong, J. L. Andres, C. Gonzalez, M. Head-Gordon, E. S. Replogle, and J. A. Pople, GAUSSIAN 98, Gaussian, Inc., Pittsburgh, PA 1998.
[20] R. S. Drago, Physical Methods for Chemists, 2nd ed., Saunders College Publishing, Orlando, FL 1992.
[21] P. Pyykkö, Mol. Phys. **99**, 1617 (2001).
[22] M. Mirzaei, N. L. Hadipour, and M. R. Abolhassani, Z. Naturforsch **62a**, 56 (2007).